Stereoselective Reductions of 3-Substituted Cyclobutanones: A Comparison between Experiment and Theory

Deraet, Xavier; Voets, Lauren; Van Lommel, Ruben; Verniest, Guido; De Proft, Frank; De Borggraeve, Wim; Alonso Giner, Mercedes

Published in:
Journal of Organic Chemistry

DOI:
10.1021/acs.joc.0c00464

Publication date:
2020

Stereoselective Reductions of 3-Substituted Cyclobutanones: a Comparison Between Experiment and Theory

Xavier Deraet,[a] Lauren Voets,[b] Ruben Van Lommel,[a,b] Guido Verniest,[c] Frank De Proft,[a*] Wim De Borggraeve,[b] Mercedes Alonso[a*]

[a] Department of General Chemistry (ALGC), Vrije Universiteit Brussel (VUB), Pleinlaan 2, 1050 Elsene, Brussels, Belgium
[b] Molecular Design and Synthesis, Department of Chemistry, KU Leuven, Celestijnenlaan 200F Leuven Chem&Tech, box 2404, 3001 Leuven, Belgium.
[c] Research group of Organic Chemistry (ORGC), Departments of Bio-engineering Sciences and Chemistry, Vrije Universiteit Brussel (VUB), Pleinlaan 2, 1050 Elsene, Brussels, Belgium

Corresponding authors: Frank De Proft (fdeprof@vub.be), Mercedes Alonso (Mercedes.Alonso.Giner@vub.be)

Abstract
The stereoselective reduction of carbonyls is of key importance in the total synthesis of natural products and in medicinal chemistry. Nevertheless, models for rationalizing the stereoselectivity of the hydride reductions of cyclobutanones towards cyclobutanols are largely lacking, unlike cyclohexanone reductions. In order to elucidate the factors that control the stereoselectivity of these reductions, we have investigated the effect of the reaction temperature, solvent, substituent and type of reducing agent using a synergistic experimental-computational approach. On the experimental side, the hydride reduction of 3-substituted cyclobutanones was proven to be highly selective for the formation of the *cis* alcohol (> 90%) irrespective of the size of the hydride reagent. The pronounced selectivity can be further enhanced by lowering the reaction temperature or decreasing solvent polarity. On the computational side, DFT and noncovalent interaction analysis reveal that torsional strain plays a major role in the preference for the anti-facial hydride approach, consistent with the Felkin-Anh model. In the presence of benzyloxy substituent, the high selectivity for the *cis* isomer is also driven by repulsive electrostatic interactions when the hydride attacks following a syn-face approach. The computed *cis*:*trans* ratios are in good agreement with the experimental ones and thus show the potential of computational chemistry for predicting and rationalizing the stereoselectivity of hydride reductions of cyclobutanones.

Introduction

The carbonyl group is a highly versatile group in organic chemistry being involved in a plethora of chemical transformations. These transformations often exploit the electrophilic character of the carbon atom of the carbonyl group, which is prone to nucleophilic additions. A textbook example of such a reaction is the addition of a hydride to a chiral cycloalkanone, resulting into a *cis:trans* mixture of cyclic alcohols (Figure 1).[1] The stereoselectivity of the hydride reduction is affected by reaction conditions such as temperature,[2-3] solvent,[4-6] bulkiness of the reducing agent[7-12] and

complexation ability of the corresponding counterion.[4,12-15] Thus, enhancing the selectivity for a given isomer can be achieved by fine-tuning these reaction conditions.

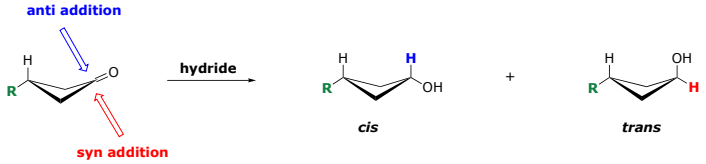

Figure 1. Schematic overview of *cis* and *trans* alcohols resulting from the anti and syn addition of the hydride to the carbonyl group with respect to the substituent R, respectively.

Stereoselectivity can be increased by lowering the reaction temperature.[2-3] Alternatively, the metal counterion of the reducing agent can modify the diastereomeric ratio based on the cation-anion association and cation-carbonyl complexation.[12-15] The former effect describes the interaction strength between the hydride and its positively charged counterion. In general, loosely bounded hydrides will be more prone to undergo a nucleophilic addition to the carbonyl group. The cation-carbonyl complexation, on the other hand, influences the reactivity by complexation between the metal counterion and the oxygen atom of the carbonyl group. Consequently, counterions that are stronger Lewis acids give rise to a carbonyl group more prone to nucleophilic additions.[12-15] Finally, the solvent influences the reactivity of the carbonyl moiety. In the specific case of borohydride reducing agents, highly polar solvent molecules compete with the oxygen of the carbonyl group to coordinate with the metal counterion, reducing therefore the cation-carbonyl complexation effect.[4-6] Accordingly, the electrophilicity of the carbonyl carbon atom decreases with increasing solvent polarity.

Although there are numerous factors influencing the facial selectivity of the hydride reduction of a carbonyl group in a chiral molecule, several explanatory stereochemical models have been proposed. For open chain compounds, the most recognized is the Felkin-Anh model,[16] in which the bulkiest or most electron-withdrawing substituent is placed orthogonally to the carbonyl moiety in a staggered conformation, in order to allow the nucleophile to attack from the least hindered side. However, this model cannot be applied to cycloalkanones as it requires free rotation around the carbon backbone to ensure the staggered conformation. Consequently, different effects have been proposed to steer the preferred facial approach of a hydride towards cyclic ketones such as: *(i)* steric hindrance and torsional strain,[16b] *(ii)* electrostatic repulsion effects,[17] *(iii)* asymmetry in π-orbitals,[18] or *(iv)* hyperconjugation.[19]

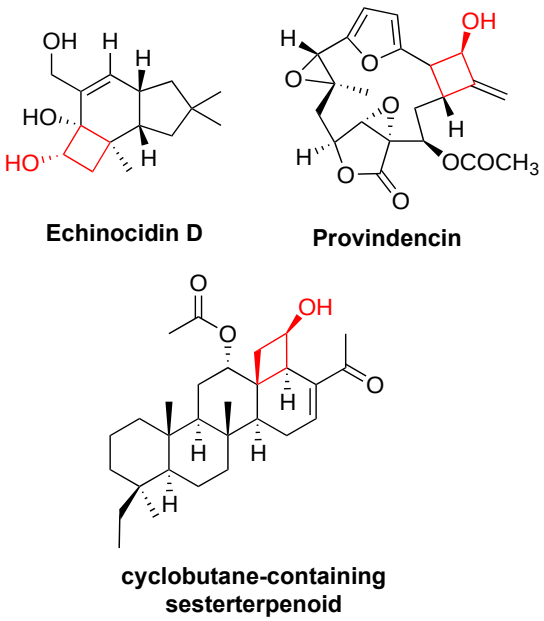

Figure 2. Examples of natural products bearing a cyclobutanol ring.

Due to the importance of the diastereomeric ratio in synthetic pathways, several models to rationalize the stereoselectivity of the reduction of substituted cyclohexanones have been proposed.[16b-19] However, the reduction of common naturally occurring small-sized four-and five-membered cycloalkanones has been investigated to a much lower extent. For cyclopentanones, the lack of models conceptualizing the preferential facial approach of a nucleophile can be justified by the rapid conformational flip of the envelope conformation, which diminishes stereoselectivity.[1] In contrast, the corresponding conformational flip of the butterfly conformation of cyclobutanones occurs at a smaller rate.[1] Furthermore, the reduction of cyclobutanones hold a prominent position in organic chemistry and the stereoselective synthesis of cyclobutanols is important in total synthesis of natural products and medicinal chemistry (Figure 2).[20] Several experimental studies indicate that the reduction of substituted cyclobutanones yields predominantly the *cis* alcohol, irrespective of the type of reducing agent (Figure 3).[21] However, unlike the reduction of cyclohexanones, a rationalization of the observed selectivity is almost never reported.

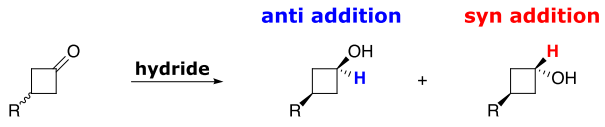

R = Ph	$LiAlH_4$	94%	6%
	L-selectride	97%	3%
R = *t*Bu	$LiAlH_4$	90%	10%
R = OBn	$NaBH_4$	98%	2%
	L-selectride	98%	2%
R = OEt	$LiAlH_4$	90%	10%

Figure 3. Experimentally observed *cis:trans* ratio for the reduction of different 3-substituted cyclobutanones with small and bulky reducing agents.

In order to elucidate the factors controlling the stereoselectivity of the hydride reduction of cyclobutanones towards cyclobutanols, we have investigated the effect of temperature, solvent, substituent on the four-membered ring and size of the reducing agent using a combined experimental-computational approach. In this study, 3-phenylcyclobutanone (**1**) and 3-benzyloxycyclobutanone (**2**) are selected as model cyclobutanones based on the different stereo-electronic effects of the substituents, their straightforward synthetic pathways and commercial availability. Experimental *cis:trans* ratios of the reduction of the corresponding 3-substituted cyclobutanones at different reaction conditions were determined by means of ^{1}H-NMR, while Density Functional Theory (DFT) calculations were employed to rationalize the stereoisomeric ratios. The computational approach was selected based on our recent benchmark study of DFT methods for describing accurately the *cis:trans* ratios of hydride reductions of 2-substituted cyclohexanones.[22] Overall, the computational study aims to rationalize the experimentally observed stereoselectivity and reveal stereo-controlling factors in the hydride reduction of chiral cyclobutanones.

Computational methodology

All quantum-chemical calculations were performed using the Gaussian quantum chemistry package (version G09.D01).[23] A two-step computational protocol was selected based on our recent benchmark of DFT approximations for describing the thermodynamics and kinetics of hydride reductions of cyclohexanones.[22] In this work, the performance of a variety of exchange correlation functionals was carefully assessed relative to canonical CCSD(T) energies. Among the tested functionals, an approach in which single-point energy calculations using the double hybrid B2PLYP-D3[24] functional on ωB97X-D[25] optimized geometries provides the most accurate transition state energies for these kinetically-controlled reactions. Accordingly, the same computational

protocol was applied to investigate the facial selectivity of hydride reductions of cyclobutanones.

All structures were computed and characterized by means of harmonic-vibrational-frequency calculations at the ωB97X-D[25]/cc-pVDZ[26] level of theory. The nature of the stationary points was assessed according to the appropriate number of negative eigenvalues of the Hessian matrix from the frequency calculations. Minima are exclusively characterized by real eigenvalues, whereas transition states exhibit exactly one negative eigenvalue corresponding to the hydride transfer. The thermodynamic contributions to the enthalpy (ΔH) and Gibbs free energy (ΔG) were computed at 1 atm for a series of reaction temperatures: 298 K, 273 K, 203 K, 195 K and 173 K. For all DFT calculations, an ultrafine grid was used to minimize the integration grid errors.[27] Subsequently, single-point energy calculations were performed at the B2PLYP-D3[24]/aug-cc-pVTZ[28] level of theory. These calculations were performed including Grimme's DFT-D3 atom-pairwise dispersion with the Becke-Johnson damping function to overcome the deficiencies of conventional functionals in the treatment of dispersion.[29] The DFT-D3 dispersion correction improves the accuracy not only for non-covalent interactions, but also for reaction barrier heights.[29] For the reductions with potassium triisopropylborohydride (KTBH), the potassium atom was described using the 6-31G(3d) basis set[30] for the geometry optimization and the 6-311+G(3df,2p)[31] basis set during the subsequent energy calculation, since the Dunning basis sets are not implemented for potassium. The remaining atoms for the KTBH-containing structures were described using the corresponding Dunning basis sets.

Implicit solvent effects were computed using the polarizable continuum model with radii and non-electrostatic terms from Truhlar and co-workers' SMD model.[32] The solvent effects for tetrahydrofuran (THF) and diethyl ether (Et_2O) were calculated at both the gas- and solvent-phase geometries at the same level of theory, resulting in solvation free energies.

Although this computational protocol is able to reproduce the experimental *cis*:*trans* ratios of hydride reductions of cyclohexanones and cyclobutanones, several hybrid functionals (B3LYP-D3,[33] M06[34] and ωB97X-D[25]) were also tested on the geometry optimization and single point energy calculations. With the exception of the popular B3LYP functional, the overall influence of the remaining methods on the structural and energetic trends appeared to be rather limited. Nevertheless, the two-step computational protocol showed the best agreement with the experimental *cis*/*trans* ratios. A more detailed description of the benchmark data can be found in the supporting information (Table S1 and Figure S1).

The theoretical ratio of *cis*:*trans* cyclobutanols was obtained through the Gibbs free energies of the different transition states ($\Delta G^{\neq}$) using a Maxwell-Boltzmann distribution at the appropriate temperature.

To assess the role of non-covalent interactions on the facial selectivity of the hydride reductions, the non-covalent interaction (NCI) index was computed on the ωB97X-D/cc-pVDZ obtained electron densities of the transition states. By plotting the reduced

density gradient (*s*) against the electron density (ρ) (Equation 1), non-covalent interactions appear as peaks at low density values due to the annihilation of the reduced density gradient at these points.[35]

$$s = \frac{1}{2(3\pi^2)^{\frac{1}{3}}} \frac{|\nabla\rho|}{\rho^{\frac{4}{3}}} \quad (1)$$

Attractive and repulsive interactions are discriminated from each other by analysing the sign of the second eigenvalue of the electron-density Hessian matrix (λ_2). A negative value of λ_2 indicates attractive interactions such as hydrogen bonding, whereas a positive value of λ_2 corresponds with repulsive interactions such as steric clashes. A great value of the NCI method lies in the visualisation of a reduced density gradient isosurface in real space, providing a three-dimensional visualisation of non-covalent interactions. Often an RGB colour scale is employed with red surfaces visualising repulsive interactions, green surfaces visualising weak attractive interactions and blue surfaces visualising strong attractive interactions. Computations of the NCI index is achieved through the NCIPLOT program,[36] while reduced gradient isosurfaces are conveniently visualised with the VMD software which is open-source for academic research purposes.[37] Importantly, the NCI is a robust technique, providing similar results regardless of the choice of method and basis set.[38]

Results and discussion

Experimental stereoselectivity for the hydride reduction of 3-substituted cyclobutanones

The influence of varying reducing agents ($LiAlH_4$, L-selectride and N-selectride) and reaction temperatures (298 K, 273 K and 195 K) on the stereoselective outcome of the reduction of 3-phenylcyclobutanone (**1**) and 3-benzyloxycyclobutanone (**2**) was experimentally assessed based on ^{1}H-NMR observed *cis:trans* ratios. The diastereomeric ratios, summarized in Table 1, were established by averaging the integration of characteristic *cis* and *trans* ^{1}H-NMR signals, as described in equation 2. By taking an average ratio over different matching *cis* and *trans* ^{1}H-NMR signals instead of a single pair of peaks, errors originating from the integration procedure or indistinguishable peak overlaps are diminished. The signal assignment for the identification of *cis*- and *trans*-3-phenylcylobutanol or *cis*- and *trans*-3-benzyloxycyclobutanol was determined using corresponding 2D-NOESY spectra cross peaks of the crude mixtures and validated based on available literature data.[21c,39] Accordingly, the signals of *cis*-3-phenylcylobutanol were assigned based on the observed cross peaks indicating coupling between H_3 (m, 3.02-2.91 ppm) and $H_{2'/4'}$ (m, 2.82-2.74 ppm), $H_{2'/4'}$ and H_1 (m, 4.33-4.24 ppm) as well as H_3 and H_1. In the case of *cis*-3-butoxycyclobutanol, cross-peaks were observed between H_3 (m, 3.67-3.56 ppm) and $H_{2'/4'}$ (m, 2.76-2.65 ppm), $H_{2'/4'}$ and H_1 (m, 3.95-3.84 ppm) as well as H_3 and H_1. All spectra including relevant peak integrations used to determine diastereomeric ratios can be consulted in the supporting information (Figure S2-S23).

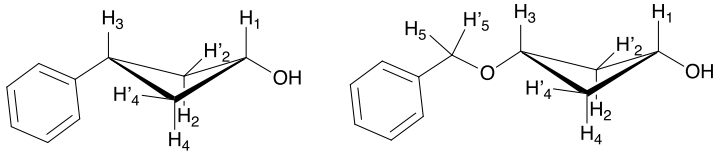

$$\%cis = \frac{1}{N}\left(\frac{\int_{cis} H_1}{\int_{cis\&trans} H_1} + \frac{\int_{cis} H_{2\&4}}{\int_{cis\&trans} H_{2\&4}} + \frac{\int_{cis} H_{2'\&4'}}{\int_{cis\&trans} H_{2'\&4'}} + \frac{\int_{cis} H_3}{\int_{cis\&trans} H_3}\right) \qquad (2)$$

From Table 1, it can be observed that for both compounds an anti-face attack of the hydride with respect to the R substituent will preferentially occur as large amounts of *cis* isomer (> 90%) are obtained, in agreement with previous reports.[21] Furthermore, as outlined in the literature, the pronounced selectivity for *cis*-3-phenylcylobutanol and *cis*-3-benzyloxycyclobutanol can be enhanced by lowering the reaction temperature.[2-3]

The reduction of 3-phenylcyclobutanone (**1**) with $LiAlH_4$ and L-selectride at 298 K gives rise to respectively 92% and 91% of *cis* product. This suggests that the use of a non-sterically hindered, weak electronegative aluminium-based or a sterically hindered, strong electronegative boron-based reducing agent does not significantly affect the selectivity. In other words, selectivity is not affected by the strength of the hydride-metal interaction. Furthermore, the results suggest that the complexation strength between the oxygen atom of the carbonyl group and the strong Li^+ Lewis acid or the weaker coordinating Na^+ does not influence the final stereoselective outcome, as the reduction of 3-benzyloxycyclobutanone (**2**) with L- or N-selectride both result in 94% of *cis*-3-benzyloxycyclobutanol. Consequently, it can be concluded that the steric bulk nor the philicity character of the reducing agent seems to influence the selectivity of cyclobutanone reductions towards the *cis* isomer. These findings are in sharp contrast with the reduction of substituted cyclohexanones, where small reducing agents give rise to the thermodynamically most advantageous isomer, while sterically hindered reagents usually yield the other isomer due to diaxial strain.[16,40]

Table 1. Overview of the experimentally obtained diastereomeric *cis:trans* ratios determined via ^{1}H-NMR for the reduction of 3-phenylcyclobutanone (**1**) and 3-benzyloxycyclobutanone (**2**) with a variety of reducing agents and different reaction temperatures.

Reducing agent	T (K)	3-phenylcyclobutanone (**1**)			3-benzyloxycyclobutanone (**2**)		
		cis	*trans*	uncertainty*	*cis*	*trans*	uncertainty*
$LiAlH_4$	298	92%	8%	± 1%	93%	7%	± 1%
	273	95%	5%	< 1%	95%	5%	± 1%
	195	97%	3%	± 1%	98%	2%	< 1%
L-selectride	298	91%	9%	< 1%	94%	6%	± 1%
	273	92%	8%	± 2%	95%	5%	± 1%
	195	95%	5%	± 1%	96%	4%	± 2%
N-selectride	298	92%	8%	± 2%	94%	6%	± 1%
	273	93%	7%	< 1%	95%	5%	± 1%
	195	98%	2%	± 1%	98%	2%	± 1%

* defined as the uncertainty on the average value.

Computational assessment of the factors influencing the stereoselective reduction of cyclobutanones

To elucidate the factors influencing the facial selectivity of the reduction of 3-phenylcyclobutanone (**1**) and 3-benzyloxycyclobutanone (**2**), a thorough computational study was undertaken. First, the role of the size of the reducing agent on the stereoselectivity was analysed. To achieve this goal, we have considered three different hydride reagents (Figure 4): lithium aluminium hydride ($LiAlH_4$), lithium triisopropylborohydride (LTBH) and sodium triisopropylborohydride (NTBH). Whereas $LiAlH_4$ represents a small hydride, TBH corresponds to a bulky hydride that mimics the reactivity of Selectride (tri-sec-butylborohydride) as for example LTBH was found to reproduce the experimental selectivities of L-Selectride,[40b] while reducing the conformational complexity and computational cost. Furthermore, different counterions of the TBH reducing reagent (Li^+ and Na^+) were considered to assess the importance of the metal counterion during the reduction. Likewise, structures containing the potassium counterion were also computed and showed fully analogous trends as compared to the other triisopropylborohydride reducing agents. However, as we did not experimentally investigate the reductions with K-selectride, the computational results for the reductions with KTBH are only reported in the supporting information (Tables S20-S24). Besides hydride bulkiness and metal complexation effects, the role of temperature and solvent on the stereoselectivity has also been considered in this study.

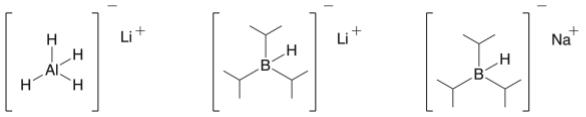

$LiAlH_4$ **LTBH** **NTBH**

Figure 4. Hydride reagents investigated in the computational work.

The mechanistic aspects of the stereoselective hydride reduction of 3-substituted cyclobutanones were studied following a similar computational approach as recently proposed for 2-substituted cyclohexanone reductions.[22] In the case of the reduction of cyclobutanone by $LiAlH_4$, the facial selectivity of the hydride attack is determined by four transition states in which the metal counterion of the reducing agent coordinates either to one (bidentate) or two hydrogen atoms (tridentate), in analogy with the mechanistic study performed by Luibrand and co-workers for the reduction of 2-substituted cyclohexanone with $LiAlH_4$ (Figure 5).[41] In the case of **TS_{cis}**, the hydride attacks from the anti-face with respect to the substituent R, which results in the *cis* cyclobutanol. In contrast, for **TS_{trans}** the hydride attacks through a syn-approach yielding the *trans* product. Structures **TS_{cis}** and **TS_{trans}** are referred to as bidentate, whereas the transition states **TS'_{cis}** and **TS'_{trans}** are tridentate. For the TBH reducing agents, only a single hydrogen atom is amenable for coordination, confining the study to the two bidentate transition structures **TS_{cis}** and **TS_{trans}**.

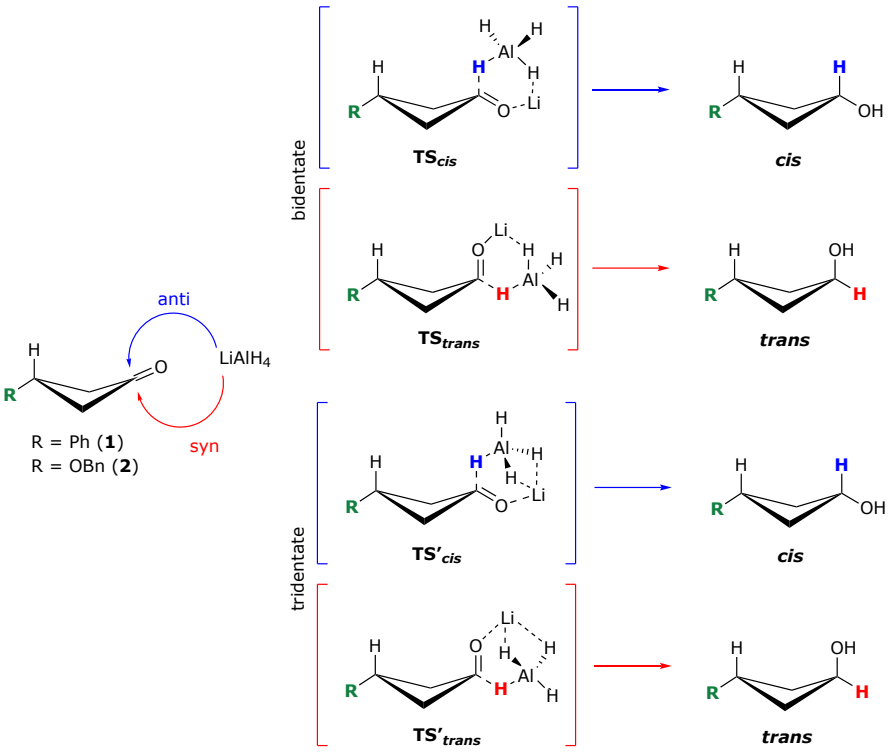

Figure 5. Schematic representation of the reactants, transition states and corresponding alcohol products involved in the reduction of 3-substituted cyclobutanones by $LiAlH_4$. **TS**$_{cis}$ and **TS´**$_{cis}$ correspond to a hydride anti-attack with respect to R resulting in the *cis* product, while **TS**$_{trans}$ and **TS´**$_{trans}$ result from the hydride syn-attack yielding the *trans* product.

Influence of the reducing agent and substituent

After optimising the transition states involved in the reduction of 3-substituted cyclobutanones (Figure 5), the impact of the reducing agent's bulk and cyclobutanone-substituent on the preference for a given transition state and hence on the stereoselectivity is computationally assessed. Relative Gibbs free energies of transition states involved in the reduction of 3-phenylcyclobutanone (**1**) and 3-benzyloxycyclobutanone (**2**) with the different reducing agents were computed at the B2PLYP-D3/aug-cc-pVTZ//ωB97X-D/cc-pVDZ level of theory and are listed in the supporting information for distinct temperatures (Tables S20-S24). Based on the relative Gibbs free energies, the *cis*:*trans* ratios were estimated using a Maxwell-Boltzmann distribution at 298K (Table 2).

Table 2. Overview of the experimental (in THF) and computational (gas phase) *cis:trans* ratios determined for the reduction of 3-substituted cyclobutanones with a variety of reducing agents at 298K.

Reducing Agent	3-phenylcyclobutanone (**1**)		3-benzyloxycyclobutanone (**2**)	
	cis:*trans* *exp.*	*cis*:*trans* *theor.*	*cis*:*trans* *exp.*	*cis*:*trans* *theor.*
$LiAlH_4$	92:8	88:12	93:7	99:1
L-selectride/LTBH	91:9	98:2	94:6	99:1
N-selectride/NTBH	92:8	82:18	94:6	95:5

Regarding the reducing agent, our experimental and computational *cis*:*trans* ratios indicate a rather small influence of the bulkiness on the facial selectivity of hydride reductions in cyclobutanones (Figures 6-7). Indeed, $LiAlH_4$, LTBH and NTBH prefer to approach the carbonyl group from the face opposite to the substituent, following an anti-facial hydride attack. Accordingly, irrespective of the size of the hydride reagent, **TS*cis*** corresponds to the lowest-energy transition structure, yielding the *cis* alcohol. Hence, both small and bulky reducing agents attack from the less sterically congested face in cyclobutanones. These findings are in sharp contrast with the reduction of cyclohexanones, in which the stereoselectivity can be reversed by using more sterically demanding reagents.[16,40] More bulky reagents usually approach the carbonyl moiety of cyclohexanone from the anti-face yielding the *cis* alcohol, while a thermodynamically controlled syn-approach of the hydride giving mainly rise to the *trans* alcohol is observed for small nucleophiles.

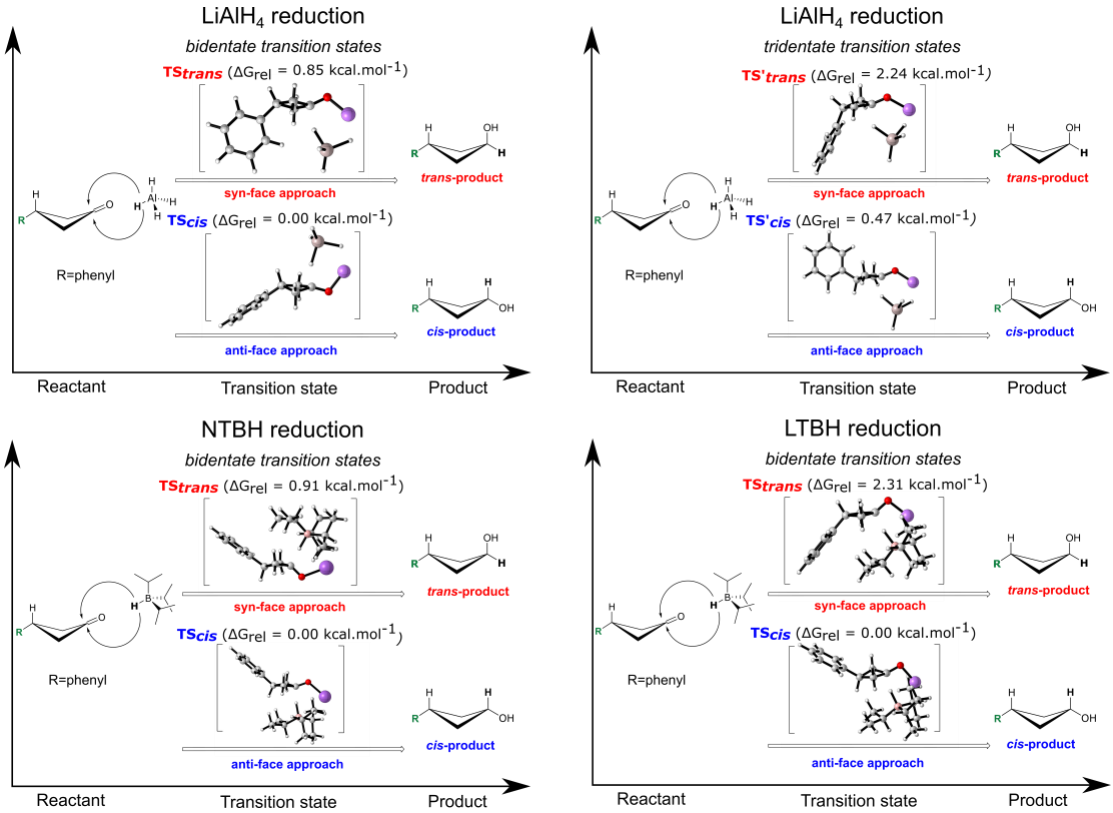

Figure 6. Schematic representation of the possible reaction paths of the reduction of 3-phenylcyclobutanone (**1**) with $LiAlH_4$ (bidentate and tridentate), NTBH (bidentate) and LTBH (bidentate). Optimized geometries of the transition states are provided together with relative Gibbs free energies computed in the gas phase at 298 K.

Table 2 indicates that the obtained Boltzmann averaged *cis*:*trans* ratios describing the reduction in gas phase at room temperature are in good agreement with the experimental ratios, both indicating a distinct preference for the formation of the *cis* alcohol. The largest dissimilarity between the experimental and computational diastereoselective ratios are retrieved for the reduction of 3-phenylcyclobutanone (**1**), being 92% with N-selectride and 82% with NTBH. We hypothesize that this difference might be ascribed to the presence of the bulkier *sec*-butyl side chains of the selectride reducing reagent used during the experiments, which completely suppresses the

possible influence of the cationic counterion. This steric effect is less pronounced for the smaller isopropyl side chains of the TBH reducing agents used for the computational modelling.

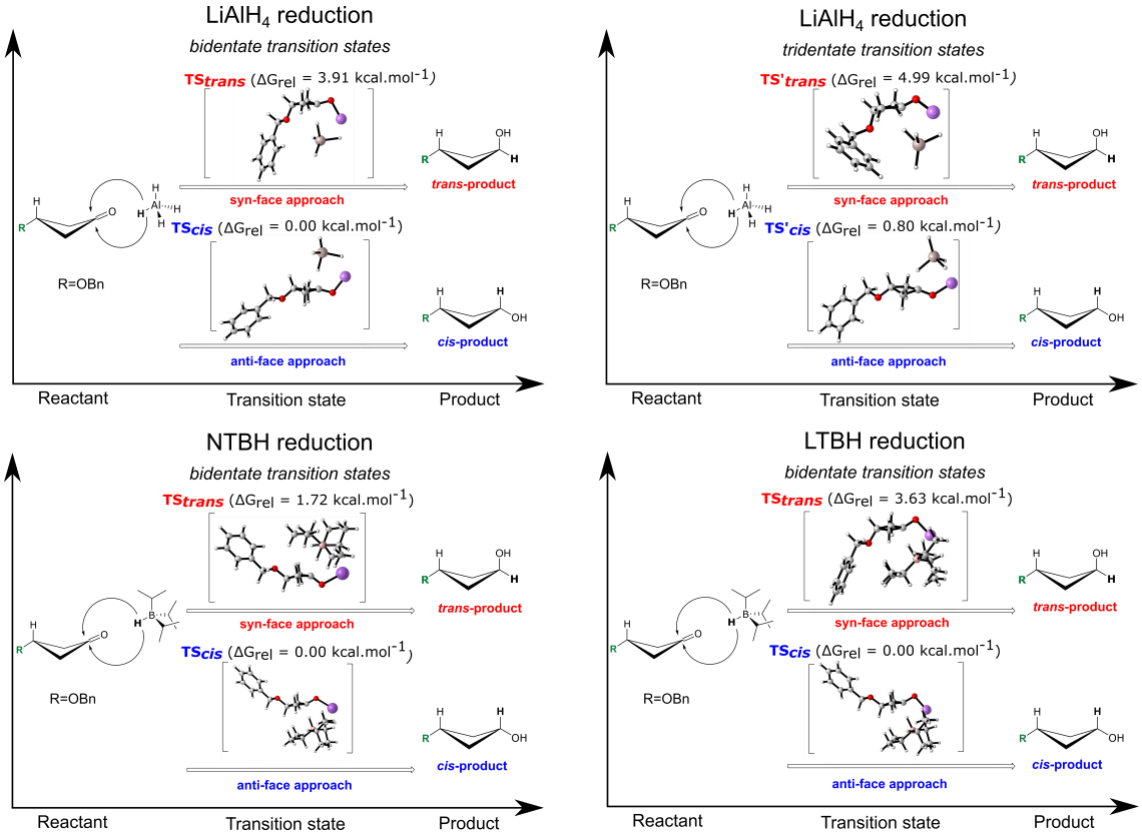

Figure 7. Schematic representation of the possible reaction paths of the reduction of 3-benzyloxycyclobutanone (**2**) with $LiAlH_4$ (bidentate and tridentate), NTBH (bidentate) and LTBH (bidentate). Optimized geometries for the transition states are provided together with relative Gibbs free energies computed in the gas phase at 298 K.

Considering the predominance of the *cis* isomer as the major product, it can be concluded that the reduction of 3-substituted cyclobutanones, irrespective of the type of reducing reagent or substituent, will preferentially occur via the $\mathbf{TS}_{cis}$ transition state. As can be observed from Figures 6 and 7, this implies that the hydride approaches the 3-substituted cyclobutanone through an anti-face Bürgi-Dunitz trajectory[42] with respect to the R-substituent. To assess the driving forces behind the clear preference for the anti-facial attack resulting in the *cis* alcohol, we focus on the comparison of the ring puckering and torsional strain of the different transition structures. This analysis is based on two structural parameters corresponding to the puckering angle (ϕ), which is defined as the angle formed by the intersection between the C_2-C_1-C_4 and C_2-C_3-C_4 planes,[43] and the dihedral angle D(O-C_1-C_2-H'$_2$) (Figure 8). The puckering angle ϕ measures the distortion of the butterfly conformation of the cyclobutanone ring, while the dihedral angle D represents the degree by which the C-H and carbonyl bonds are eclipsed. To quantify the structural distortion induced by the hydride attack, the structural parameters of the initial reagents were taken as a reference. The puckering angle (ϕ) and the dihedral angle (D) are 17.1° and 82.6° for

3-phenylcyclobutanone, while for 3-benzyloxycyclobutanone these respective angles are 16.5° and 84.6°. An increase in ϕ with respect to the reference values is linked to a decrease in torsional strain, while the four-membered ring becomes more puckered. In this regard, it is important to note that cyclobutanone represents an example of an extremely fine balance between angle and torsional strain.[43] Puckering of the cyclobutanone ring decreases the torsional strain associated with eclipsed interactions, while increasing the angle strain caused by the compression of C-C-C bond angles. Because the decrease in torsional strain is greater than the increase in angle strain, the puckered conformation is more stable than the planar one in cyclobutanones. On the other side, a more staggered conformation is obtained as the dihedral angle *D* becomes closer to 60°, and, accordingly, a decrease in *D* indicates a reduced torsional strain as the carbonyl bond and the neighbouring CH bond becomes less eclipsed (Figure 8). The different structural parameters for the different transition states are summarized in Table 3.

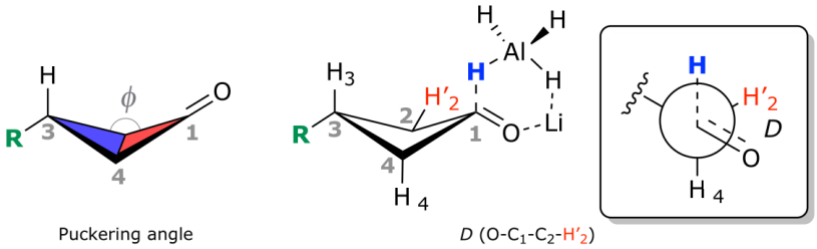

Figure 8. Measurement of the ring puckering and torsional strain in the transition structures of hydride addition to cyclobutanones.

Table 3. Relative Gibbs free energies (in kcal mol^{-1}) calculated in the gas phase at 298 K together with selected torsional parameters (ϕ and *D* in °) for the different transition states involved in the reduction of 3-phenyl- and 3-benzyloxycyclobutanone with $LiAlH_4$.

	3-phenylcyclobutanone (**1**)					3-benzyloxycyclobutanone (**2**)				
$LiAlH_4$	ref[a]	**TS_{cis}**	**TS_{trans}**	**TS'_{cis}**	**TS'_{trans}**	ref[a]	**TS_{cis}**	**TS_{trans}**	**TS'_{cis}**	**TS'_{trans}**
ΔG_{rel}	-	0.00	1.04	0.47	2.32	-	0.00	3.91	0.80	4.99
ϕ	17.1	20.3	2.2	20.1	17.1	16.5	20.1	17.6	19.8	14.6
D	82.6	73.4	100.1	77.4	77.6	84.6	72.7	75.8	76.7	81.4

[a] The reference values correspond to the reactant 3-substituted cyclobutanone.

As can be inferred from Table 3, the preference for anti-facial addition pathways for the reduction of 3-phenylcyclobutanone (**1**) with $LiAlH_4$ can be fully attributed to a reduction in torsional strain. Indeed, the puckering angle for the preferred transition states **TS_{cis}** and **TS'_{cis}** increases by approximately 3° with respect to the initial angle of reactant **1**, while the dihedral angle *D* decreases indicating that the carbonyl bond and the neighbouring C-H bond are less eclipsed. This decrease is more pronounced (ΔD = -9.2°) in the case of the bidentate transition state **TS_{cis}** as compared to its tridentate **TS'_{cis}** analogue, which can explain the small difference in Gibbs free energy between both structures (+0.47 kcal mol^{-1}). In contrast to transition state **TS_{cis}**, the less favourable syn-face approach via **TS_{trans}** results in a pronounced decrease in the puckering angle ϕ, adopting a quasi-planar squared geometry characterized by high torsional strain. Consequently, our calculations support that torsional strain plays a major role in the preference for an anti-facial addition pathway in the reduction of 3-phenylcyclobutanone (**1**) with $LiAlH_4$, leading to a high population of the *cis* isomer

(88%), which is in very good agreement with our experimental ratio. These findings support the Felkin-Anh model,[16] which is based on the torsional strain of the transition states for nucleophilic additions to cycloalkanones.

For the $LiAlH_4$ reduction of 3-benzyloxycyclobutanone (**2**), our calculations support almost full stereoselectivity towards the *cis* product (99%). Again, the largest increase in ring puckering and concomitant reduction in *D* is observed for $\mathbf{TS}_{cis}$ ($\Delta\phi$ = +3.6°, ΔD = -11.9°). Nevertheless, the syn-facial attack of the hydride via $\mathbf{TS}_{trans}$ also involves a relief of torsional strain, but to a lesser extent ($\Delta\phi$ = +1.1°, ΔD = -8.8°). As the energy difference between $\mathbf{TS}_{cis}$ and $\mathbf{TS}_{trans}$ amounts to 3.9 kcal mol^{-1}, it is likely that the relief of torsional strain is not the sole driving force behind the observed stereoselectivity for the $LiAlH_4$ reduction of 3-benzyloxycyclobutanone (**2**).

In order to further explain the stereoselectivity of the reduction of **2**, it is necessary to look beyond changes in structural parameters. For this reason, the role of non-covalent interactions is assessed using the non-covalent interaction (NCI) index.[35] The latter allows to distinguish attractive and repulsive non-covalent interactions based on a 2-dimensional plot of the reduced density gradient (*s*) with respect to the electron density (ρ) multiplied by the sign of the second eigenvalue of the electron density Hessian matrix (λ_2). Peaks appearing at negative values of $\rho\text{sign}(\lambda_2)$ indicates an attractive non-covalent interaction, while a peak at a positive value indicates a repulsive interaction. Additionally, a 3-dimensional representation of the non-covalent interactions is provided by visualizing isosurfaces of *s* with an RGB colour scale indicating repulsive interactions as red surfaces, weak attractive interactions as green surfaces and strong attractive interactions as blue surfaces.

Based on the 2-dimensional plots comparing the attractive and repulsive non-covalent interactions occurring during an anti-facial ($\mathbf{TS}_{cis}$) or syn-facial ($\mathbf{TS}_{trans}$) approach of $LiAlH_4$ towards 3-benzyloxycyclobutanone (**2**) (Figure 9), it can be observed that $\mathbf{TS}_{trans}$ is characterized by more pronounced repulsive interactions, *i.e.* significant more peaks are observed with a positive value of $\text{sign}(\lambda_2)\rho$, as compared to $\mathbf{TS}_{cis}$. The gradient isosurfaces allow us to assign these repulsive interactions in $\mathbf{TS}_{trans}$ to the presence of an additional interaction between the benzyloxy-substituent and the AlH_4^- moiety. The latter can be assigned to a repulsive electrostatic interaction induced by the proximity of the electronegative oxygen atom of the OBn substituent and the reducing agent. As this interaction is not present during the anti-facial attack ($\mathbf{TS}_{cis}$) of $LiAlH_4$, we conclude that the strong preference for $\mathbf{TS}_{cis}$ in the reduction of 3-benzyloxycyclobutanone (**2**) with $LiAlH_4$ arose from the relief of torsional strain and repulsive interactions of the incoming hydride with the benzyloxy substituent.

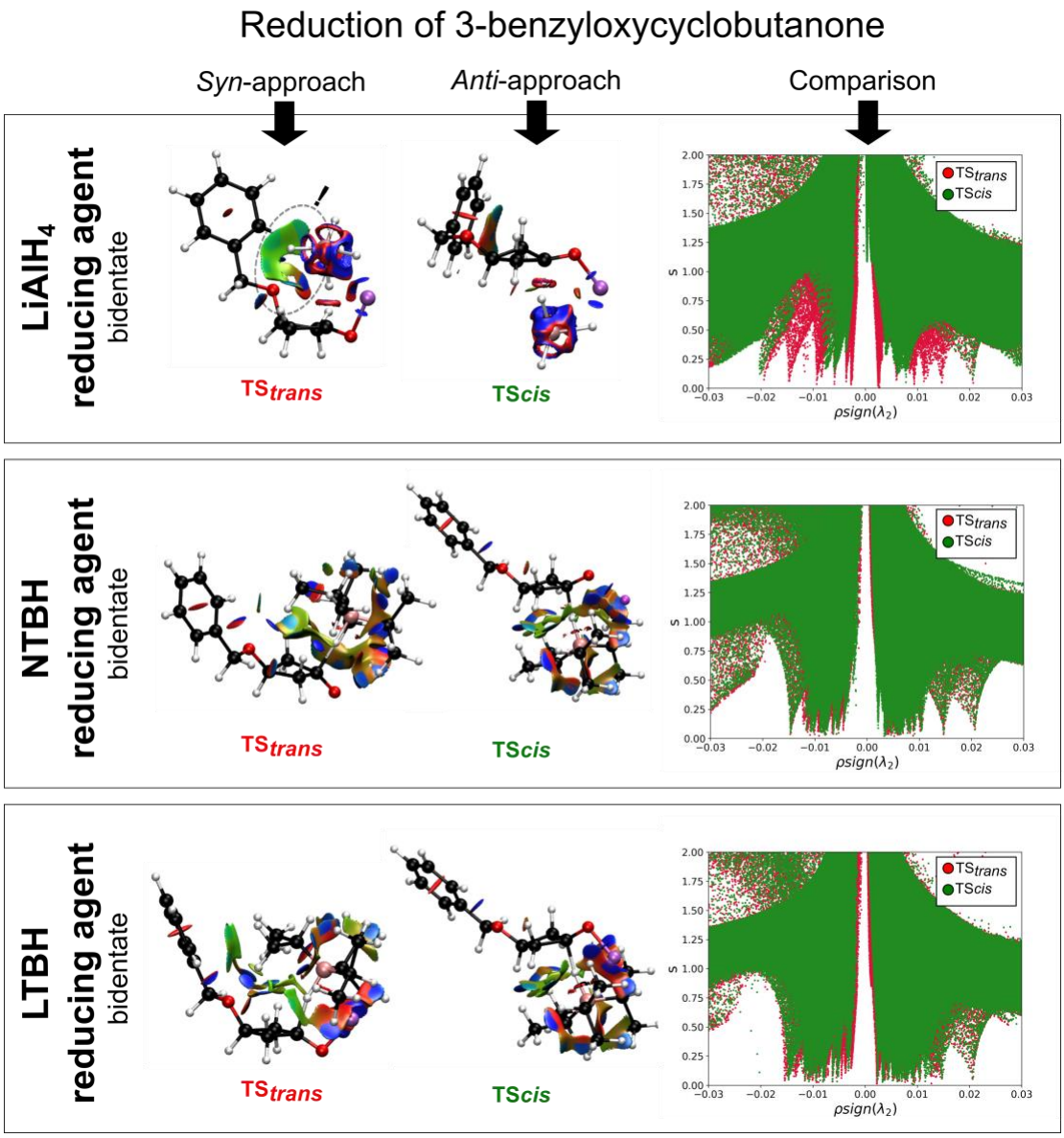

Figure 9. Non-covalent interactions present in the various transition states describing the reduction of 3-benzyloxycyclobutanone (**2**) with $LiAlH_4$, NTBH and LTBH. The gradient isosurfaces (s = 0.5) are coloured on a RGB scale according to sign(λ_2)ρ over the range -0.01 a.u. to 0.01 a.u. Plots of the reduced density gradient *vs* the electron density multiplied by the sign of the second Hessian eigenvalue (λ_2). Key interactions are highlighted with a circle.

In contrast to the reduction of 3-benzyloxycyclobutanone (**2**), the stereochemical outcome of the reduction of 3-phenylcyclobutanone (**1**) with $LiAlH_4$ does not appear to be influenced by non-covalent interactions. Accordingly, the 2-dimensional plots of the reduction of **1** with $LiAlH_4$ clearly show that the difference in repulsive and attractive signals between $\mathbf{TS}_{cis}$ and $\mathbf{TS}_{trans}$ is rather small (Figure 10), even for the tridentate transition states $\mathbf{TS'}_{cis}$ and $\mathbf{TS'}_{trans}$. Therefore, it can be concluded that while the reduction of 3-phenyl- and 3-benzyloxycyclobutanone with $LiAlH_4$ yields predominantly the *cis* alcohol, their stereoselectivity is driven by different factors. For the 3-phenylcyclobutanone, stereoselectivity is solely driven by the reduction of torsional strain during the anti-facial attack, while for 3-benzyloxycyclobutanone,

besides torsional strain, electrostatic repulsive interactions between the hydride and the OBn substituent also plays an important role.

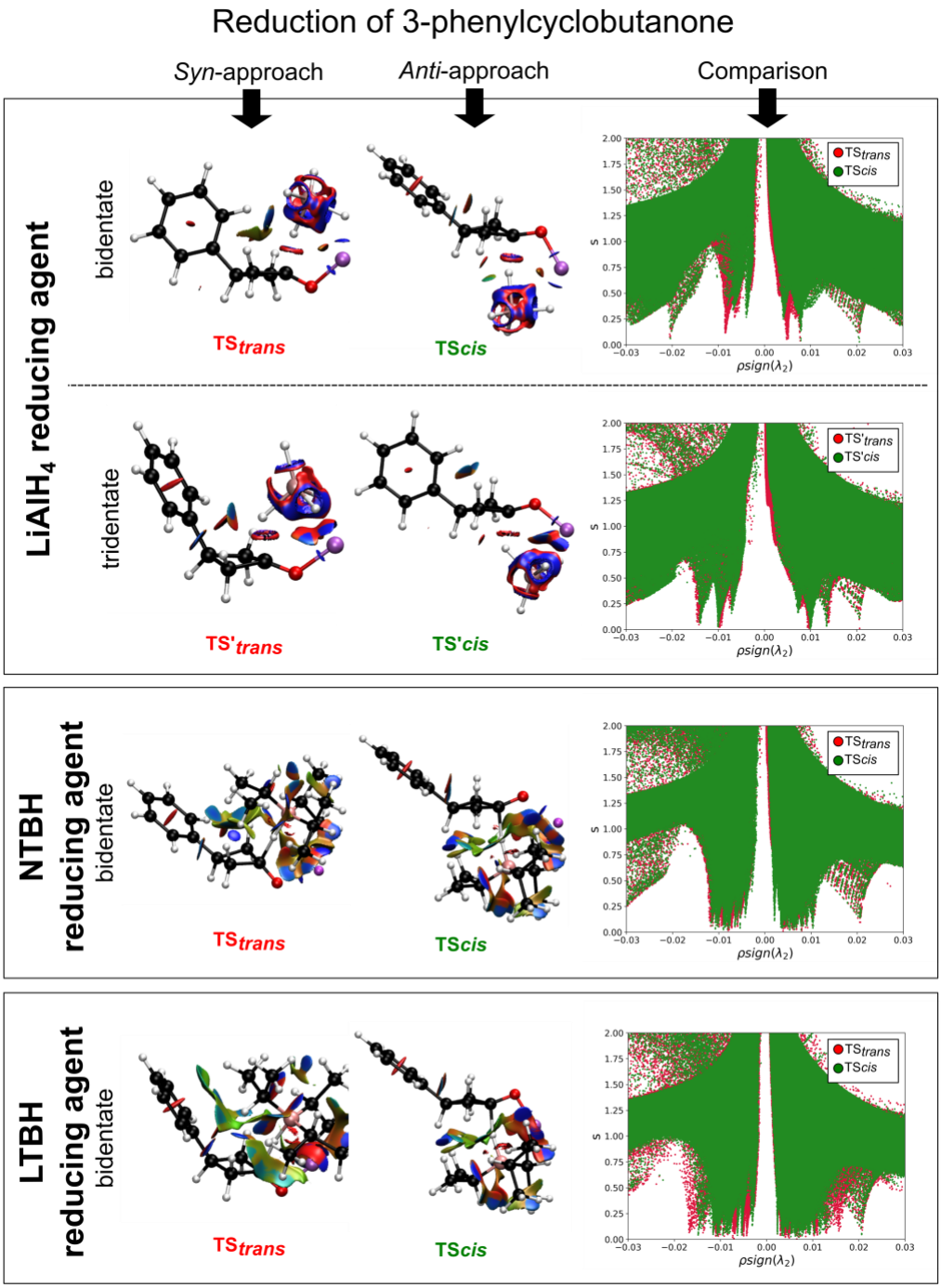

Figure 10. Non-covalent interactions present in the various transition states describing the reduction of 3-phenylcyclobutanone with $LiAlH_4$, NTBH and LTBH. The gradient isosurfaces (s = 0.5) are coloured on a RGB scale according to sign(λ_2)ρ over the range -0.01 a.u. to 0.01 a.u. Plots of the reduced density gradient *vs* the electron density multiplied by the sign of the second Hessian eigenvalue (λ_2).

Reduction with bulky reducing agents

Having assessed the driving factors behind the stereoselectivity of the cyclobutanone reduction with the small reducing agent $LiAlH_4$, we focus now on the influence of bulkiness of the hydride reagent. Accordingly, we have investigated the reduction of **1** and **2** with bulkier triisopropylborohydride (TBH) reducing agents. As shown in Table 2, overall the computed *cis*:*trans* ratios for reductions with TBH reagents compare well with the experimental diastereomeric ratios for reductions with bulkier selectrides. As mentioned before, the largest discrepancy between the TBH computed ratios and the experimental selectride ratios are observed for the reduction of 3-phenylcyclobutanone (**1**) with NTBH (92:8 and 82:18, respectively). We hypothesize that this could be explained by the steric bulk of the *sec*-butyl side chains of the selectride reagents which completely suppresses the coordinating effect of the Na^+ counterion with the oxygen of the carbonyl group. The smaller isopropyl side chains of the TBH reducing agent possibly does not succeed in reproducing this effect. With this in mind, we believe that when using less sterically demanding reducing reagents (*e.g.* TBH) the Lewis acid character of the counterion also affects the stereoselectivity of the reduction, as our calculations show that that the percentage of the *cis* product decreases from 98% to 82% when going from LTBH (Li^+) to NTBH (Na^+). This statement is consistent with experimental observations on reductions of cyclic and acyclic ketones with Na- and Li-based reducing agents, in which the latter also gives higher stereoselectivity.[44] When more sterically demanding hydride reagents are used (*e.g.* selectride), the counterion effect diminishes and a similar stereoselectivity is observed regardless of the counterion of the reducing agent.

Table 4. Relative Gibbs free energies (in kcal mol^{-1}) together with selected torsional parameters (ϕ and *D* in °) for the different transition states involved in the reduction of 3-phenyl- and 3-benzyloxycyclobutanone with LTBH and NTBH.

	3-phenylcyclobutanone (**1**)			3-benzyloxycyclobutanone (**2**)		
LTBH	ref[a]	TS_{cis}	TS_{trans}	ref[a]	TS_{cis}	TS_{trans}
ΔG_{rel}	-	0.00	2.38	-	0.00	3.63
ϕ	17.1	16.4	3.4	16.5	15.5	2.0
D	82.6	84.6	102.9	84.6	83.9	101.6
NTBH	ref[a]	TS_{cis}	TS_{trans}	ref[a]	TS_{cis}	TS_{trans}
ΔG_{rel}	-	0.00	0.91	-	0.00	1.72
ϕ	17.1	14.4	21.1	16.5	13.4	17.8
D	82.6	85.9	126.8	84.6	85.5	124.6

[a] The reference values correspond to the reactant 3-substituted cyclobutanone.

In the case of LTBH, we observe that both syn- and anti-facial addition increases the torsional strain with respect to the starting cyclobutanone, but this increase is significantly larger for transition state $\mathbf{TS}_{trans}$ as revealed by the puckering and *D* angles. It is noteworthy that the cyclobutanone ring adopts a quasi-planar geometry in $\mathbf{TS}_{trans}$ and a puckered conformation in $\mathbf{TS}_{cis}$. Consequently, torsional strain appears to be again the main driving force for the observed stereoselectivity of the reduction of **1** and **2** with LTBH.

For the reduction with NTBH, the differences in the puckering angle between $\mathbf{TS}_{cis}$ and $\mathbf{TS}_{trans}$ are smaller, with the four-membered ring being more puckered in $\mathbf{TS}_{trans}$. This

would explain the minor energy differences between $\mathbf{TS}_{cis}$ and $\mathbf{TS}_{trans}$ for the reductions with NTBH. However, *D* indicates that the carbonyl group is almost eclipsed by the C(2)-H bond in $\mathbf{TS}_{trans}$ (*D* ~ 125°), whereas a more staggered arrangement is observed in $\mathbf{TS}_{cis}$ (*D* ~ 86°). This torsional strain is then relieved in the anti-facial attack, which explain the preference for $\mathbf{TS}_{cis}$ according to the relative Gibbs free energies. Furthermore, no significant differences are observed between the 2-dimensional plots of $\mathbf{TS}_{cis}$ and $\mathbf{TS}_{trans}$ for the reduction of **1** and **2** with both LTBH and NTBH (Figures 9 and 10), suggesting a minor influence of repulsive electrostatic interactions on the preference for $\mathbf{TS}_{cis}$. Consequently, the preference for the anti-facial attack by bulkier LTBH and NTBH is mainly driven by the lower torsional strain than the syn-facial attack.

Effect of temperature and solvent

Besides stereo-determining effects of the substituent and the reducing agent, the choice of appropriate reaction conditions is also important for the stereochemical outcome of hydride reductions of 3-substituted cyclobutanones, as shown in the experimental section. Consequently, the influence of the reaction temperature and solvent on the reduction of 3-phenyl- and 3-benzyloxycyclobutanone was investigated computationally. The corresponding *cis*:*trans* ratios obtained for different temperatures and solvent environments are summarized Table 4 and Table 5, respectively. An enhanced stereoselectivity by lowering the reaction temperature during hydride reductions[2-3] is well known and also holds for the reduction of cyclobutanones, as both experimental and computational ratios reveal an increase in preference towards the *cis* product when the reaction is performed at 195K. In other words, this indicates that transition state $\mathbf{TS}_{cis}$ involving an anti-facial attack of the hydride on the cyclobutanone becomes energetically more favoured than transition state $\mathbf{TS}_{trans}$ upon lowering the temperature, stemming from the lower entropy of $\mathbf{TS}_{cis}$ compared to $\mathbf{TS}_{trans}$ (G=H-TS).

Table 4. Overview of the experimental (in THF) and computational (gas phase) *cis:trans* ratios determined for the reduction of 3-substituted cyclobutanones with a variety of reducing agents at 298, 273 and 195 K.

Reducing Agent	Reaction temperature (K)	3-phenylcyclobutanone (**1**)		3-benzyloxycyclobutanone (**2**)	
		cis:*trans* *exp*.	*cis*:*trans* *theor*.	*cis*:*trans* *exp*.	*cis*:*trans* *theor*.
$LiAlH_4$	298	92:8	88:12	93:7	99:1
	273	95:5	91:9	95:5	99:1
	195	97:3	97:3	98:2	99:1
L-selectride LTBH	298	91:9	98:2	94:6	99:1
	273	92:8	99:1	95:5	99:1
	195	95:5	99:1	96:4	99:1
N-selectride NTBH	298	92:8	82:18	94:6	95:5
	273	93:7	85:15	95:5	96:4
	195	98:2	93:7	98:2	98:2

The impact of solvation was determined using solvation Gibbs free energies computed with the implicit SMD model for THF and Et_2O on both gas phase as well as on solvent-optimised geometries. The influence of optimizing the different transition structures

in solvent on the structural parameters and Gibbs free energies is summarized in Table S26 of the supporting information. Regarding the structural parameters, the solvent effects on the puckering angle ϕ and the dihedral angle *D* appears to be rather limited. Indeed, ϕ of the solvent-optimized transition states involved in the reduction with $LiAlH_4$ and LTBH agent differs from the gas phase geometry by an average of 0.78°, while almost identical averaged differences, *i.e.* 0.80°, are observed in the case of the bulky LTBH agent. Similarly, the extent to which solvent affects the degree by which the CH_2 and carbonyl bonds are eclipsed, as measured by the dihedral angle *D*, is rather small. Regarding the energies, both methodologies indicate a clear preference for transition state $\mathbf{TS}_{cis}$, in line with the predominant *cis* alcohol. Nevertheless, optimization in solvent reduces the Gibbs free energy difference between the bidentate transition states ($\mathbf{TS}_{cis}$ and $\mathbf{TS}_{trans}$) by an average of 1.1 kcal mol^{-1}, while a further destabilization of the tridentate transition states (~ 1 kcal mol^{-1}) relative to their bidentate analogues is observed for the reductions with $LiAlH_4$. These energy changes translate into an average difference of 2.5% in the amount of *cis* alcohol between gas and solvent phase optimised structures. Despite the minimal influence of implicit solvation on the geometries and energies, the computed *cis*:*trans* ratios for the reduction in THF agrees better with the experimental ones upon optimization of the transition structures in solvent (Table S27).

The *cis*:*trans* ratios computed for the different reductions in gas phase, THF and diethyl ether (Table 5) indicate that the polarity of the solvent might also affect the population of the *cis* product. As such, a higher selectivity is observed for the cyclobutanone reductions when using less-polar solvents, such as Et_2O. Thus, selectivity increases as the solvent polarity decreases, according to the computational data. As such, an increase by 3 to 4% in the *cis* isomer population is observed for $LiAlH_4$ reductions when going from THF to Et_2O, while only a difference of 2% between both solvents is observed for reductions with bulky TBH agents. We therefore hypothesise that the more polar THF molecules might compete with the oxygen of the carbonyl group to coordinate with the metal counterion. Accordingly, the electrophilicity of the carbonyl carbon atom decreases with increasing solvent polarity. However, a more accurate description of the solvent effect requires the use of explicit solvation models.[45]

Table 5. Overview of the computational *cis:trans* ratios determined for the reduction of 3-substituted cyclobutanones in gas phase, THF and Et_2O (solvent-optimised geometries) with a variety of reducing agents at 298K.

Reducing Agent	Solvent	3-phenylcyclobutanone (**1**) *cis*:*trans* *theor.*	3-benzyloxycyclobutanone (**2**) *cis*:*trans* *theor.*
$LiAlH_4$	Gas	88:12	99:1
	THF	90:10	94:6
	Et_2O	93:7	98:2
LTBH	Gas	98:2	100:0
	THF	94:6	99:1
	Et_2O	96:4	100:0
NTBH	Gas	82:18	95:5
	THF	88:12	99:1
	Et_2O	93:7	96:4

Conclusion

Since models for rationalizing the facial selectivity of hydride reductions of cyclobutanones towards cyclobutanols are largely lacking, we have investigated the effect of substituent, reducing agent, temperature and solvent on the stereoselectivity of such reductions using a synergistic experimental-computational approach. The experimental and computational results indicate that the reduction of 3-substituted cyclobutanones is highly stereoselective for the formation of the *cis* alcohol, irrespective of the size of the hydride reagent or reaction conditions. Nevertheless, the stereoselectivity can be further enhanced by lowering the reaction temperature or solvent polarity. Unlike the extensively investigated reductions of cyclohexanones, neither steric effects nor the strength of the hydride donor or cationic counterion of the reducing agent appeared to have a substantial influence on the stereoselectivity. Through DFT calculations and the NCI index, the preference for the *cis* isomer was rationalized. The computational results indicate that the reduction with small and bulky hydride reagents preferentially occurs through a bidentate transition state, in which the hydride approaches the carbonyl functionality from the opposite side as the substituent, thereby yielding the *cis* isomer. Torsional effects are shown to play a major role in the preference for the anti-facial approach, consistent with the Felkin-Anh model. Furthermore, the high selectivity of the $LiAlH_4$ reduction of 3-benzyloxycyclobutanone is also driven by minimising the repulsive electrostatic interactions of the incoming hydride and the OBn substituent. With a bulky reducing agent, the preference for the anti-facial attack is mainly driven by the lower torsional strain as compared to a syn-facial approach. Our study demonstrates the potential of DFT and non-covalent interaction analysis to elucidate the factors controlling the high stereoselectivity of hydride reductions of cyclobutanones, providing *cis*:*trans* ratios in good agreement with our experimental results.

Experimental Procedure

NMR Spectroscopy

^{1}H-NMR spectra were recorded on a Bruker Avance III HD 400 (at 400 MHz) spectrometer. Samples were dissolved either in $CDCl_3$ (7.26 ppm, singlet) or DMSO-d_6

(2.50 ppm, quintet), while tetramethylsilane was used as an internal standard. All spectra including the relevant peak integrations used to determine diastereomeric ratios are provided in the supporting information.

Chromatography

TLC analysis was performed using Sigma-Aldrich 20 x 20 cm precoated glass TLC plates with fluorescent indicator at 254 nm (article number 99571: layer thickness 250 µm, particle size 8.0-12.0 µm, average pore diameter 60 Å). Visualization of the products and their fluorescence features were achieved by UV-radiation at 254 nm.

Flash column chromatography (MPLC) was performed using a Büchi Sepacore® flash system, consisting of a Büchi C-660 Fraction Collector, a Büchi C-615 Pump Manager, a Knauer WellChrom K-2501 spectrophotometer (working at 254 nm), two Büchi C-605 Pump Modules and a Linseis D120S plotter. Büchi PP cartridges (12/150 mm) were filled with 8 g of Acros ultra-pure silica gel for column chromatography (article number 360050300: particle size 40-60 µm, average pore diameter 60 Å) using a Büchi C-670 Cartridger.

All procedures were carried out under nitrogen atmosphere and in flame-dried glassware. All chemicals were obtained from available sources (Fluorochem and Sigma Aldrich®) and were used without any further purification. Solvents were bought dry and for THF an additional drying process is performed by using a MBRAUN MB-SPS-800 Solvent Purification System. Deuterated solvents were bought dry and additionally dried with molecular sieves. The authors note that it is crucial to work under dry conditions for safety reasons, as hydride reduction agents are well known to react violently with water. In the case of $LiAlH_4$ reaction with water results in the formation of flammable hydrogen gas. For this reason, we advise to use premade solutions of the hydride reducing agent instead of the pure reagent if possible.

Reduction procedure A with $LiAlH_4$. Into a two-necked flask of 50 mL, equipped with a magnetic stirring bar, a septum and a balloon, 1.0 equivalent (0.6 mmol) of the cyclobutanone was suspended into 11 mL of dry THF. Subsequently, the reaction mixture was cooled to the desired temperature (-78°C, 0°C or room temperature). Next, 1.2 equivalents of the reducing agent in solution (1.0 M in THF) (0.72 mmol) was added dropwise to the reaction mixture at the appropriate temperature. The solution was stirred for 4h at the desired temperature. Upon completion of the reaction, anhydrous acetone (6 mL) was added, and stirring was continued for 5 min. The cooling bath (if present) was removed, 15 mL of aqueous saturated NH_4Cl was slowly added to the reaction mixture. The mixture was stirred for another 1h at room temperature. Afterwards the organic material was extracted with ethyl acetate. The organic layers were combined and dried over $MgSO_4$, filtered and the solvent was removed under reduced pressure. Crude (except otherwise stated) NMR measurements were performed to determine the diastereomeric ratios of the cyclobutanol.

Reduction procedure B with L-selectride. Into a two-necked flask of 50 mL, equipped with a magnetic stirring bar, a septum and a balloon, 1.0 equivalent (0.6 mmol) of the

cyclobutanone was suspended into 11 mL of dry THF. Subsequently, the reaction mixture was cooled to the desired temperature (-78°C, 0°C or rt). Next, 1.2 equivalents of the reducing agent in solution (1.0 M in THF) (0.72 mmol) was added dropwise to the reaction mixture at the appropriate temperature. The solution was stirred for 4h at the desired temperature. Upon completion of the reaction, anhydrous acetone (6 mL) was added, and stirring was continued for 5 min. The cooling bath (if present) was removed, 15 mL of aqueous saturated NH_4Cl was slowly added to the reaction mixture. The mixture was stirred for another 1h at room temperature. Afterwards the organic material was extracted with ethyl acetate. The organic layers were combined and dried over $MgSO_4$, filtered and the solvent was removed under reduced pressure. Crude (except otherwise stated) NMR measurements were performed to determine the diastereomeric ratios of the cyclobutanol.

Reduction procedure C with L-/N-selectride. Into a two-necked flask of 50 mL, equipped with a magnetic stirring bar, a septum and a balloon, 1.0 equivalent (0.6 mmol) of the cyclobutanone was suspended into 11 mL of dry THF. Subsequently, the reaction mixture was cooled to the desired temperature. Next, 1.2 equivalents of the reducing agent in solution (1.0 M in THF) (0.72 mmol) was added dropwise to the reaction mixture at the appropriate temperature. The solution was stirred for 4h at the desired temperature. Upon completion of the reaction, the reaction mixture was quenched with water (1 mL), ethanol (4 mL) and 3M NaOH (4 .5 mL). The mixture was cooled to 0 °C and a solution of H_2O_2 (4 mL, 30% in H_2O) was cautiously added. After addition the reaction mixture was brought to room temperature and stirred for 1h. Next, the organic material was extracted with diethyl ether and washed with water, brine and aqueous $NaHCO_3$. The organic layers were combined and dried over $MgSO_4$, filtered and the solvent was removed under reduced pressure. Crude (except otherwise stated) NMR measurements were performed to determine the diastereomeric ratios of the cyclobutanol.

Characterization of *cis*-3-phenylcyclobutanol: **^{1}H-NMR** (400 MHz, $CDCl_3$) δ 7.34-7.16 (m, Phenyl), 4.34-4.24 (m, H_1), 3.02-2.91 (m, H_3), 2.82-2.74 (m, $H_{2'}$ & $H_{4'}$), 2.07-1.97 (m, H_2 & H_4), 1.79 (br s, OH).
Characterization of *trans*-3-phenylcyclobutanol: **^{1}H-NMR** (400 MHz, $CDCl_3$) δ 7.34-7.16 (m, Phenyl), 4.59-4.52 (m, H_1), 3.68-3.59 (m, H_3), 2.55-2.38 (m, $H_{2'}$ & $H_{4'}$ & H_2 & H_4), 1.79 (br s, OH).
Characterization of *cis*-3-benzyloxycyclobutanol: **^{1}H-NMR** (400 MHz, $CDCl_3$) δ 7.37-7.26 (m, Phenyl), 4.42-4.39 (m, H_5 & $H_{5'}$), 3.95-3.84 (m, H_1), 3.76-3.56 (m, H_3), 2.76-2.65 (m, $H_{2'}$ & $H_{4'}$), 1.98-1.89 (m, H_2 & H_4), 1.87* (br s, OH).
Characterization of *trans*-3-benzyloxycyclobutanol: **^{1}H-NMR** (400 MHz, $CDCl_3$) δ 7.37-7.26 (m, Phenyl), 4.57-4.50 (m, H_1), 4.42-4.39 (m, H_5 & $H_{5'}$), 4.32-4.24 (m, H_3), 2.41-2.32 (m, $H_{2'}$ & $H_{4'}$), 2.22-2.13 (m, H_2 & H_4), 1.87* (br s, OH).

Supporting Information

* ppm-value when $LiAlH_4$ is used as reducing agent, 2.64 ppm (L-selectride), 1.80 ppm (N-selectride)

The NOESY spectra and ^{1}H-NMR spectra, DFT benchmark study, Boltzmann averaged *cis*:*trans* ratios, relative electronic and Gibbs free energies for different temperatures and reducing agents, implicit solvation energies using gas-phase and solvent-phase geometry optimisation, XYZ coordinates of optimised transition states.

Acknowledgements

The authors wish to thank the Fund for Scientific Research – Flanders (FWO) and the Vrije Universiteit Brussel (VUB) for their continuous support. F.D.P. acknowledges the VUB for a Strategic Research Program awarded to his research group. M. A. thanks the FWO for a postdoctoral fellowship (12F4416N) and the VUB for financial support. R. V. L. acknowledges the FWO for a predoctoral fellowship received (1185219N). Computational resources and services were provided by the Shared ICT Services Centre funded by the Vrije Universiteit Brussel, the Flemish Supercomputer Center (VSC) and FWO. The graphical representations of the geometries were obtained using the freely available CYLview[46] software.

References

(1) Clayden, J.; Greeves, N.; Warren, S. Stereoselectivity in cyclic molecules. *Organic Chemistry;* 2nd edition; Oxford University Press: New York, 2012; pp 1512.

(2) Ward, D.E.; Rhee, C.K. Chemoselective reductions with sodium-borohydride. *Can. J. Chem.* **1989**, *67*, 1206-1211.

(3) (a) Cainelli, G.; Giacomini, D.; Galletti, P. Temperature and solvent effects in facial diastereoselectivity of nucleophilic addition: entropic and enthalpic contribution. *Chem. Commun.* **1999**, *7*, 567-572. (b) Cainelli, G.; Giacomini, D.; Galletti, P.; Quintavalla, A. Solvent and temperature effects on diastereofacial selectivity: amines as co-solvents in n-butyllithium addition to α-chiral aldehydes. *Eur. J. Org. Chem.* **2003**, *10*, 1993.

(4) Brown, H.C.; Narasimhan, S.; Choi, Y.M. Selective reductions .30. effect of cation and solvent on the reactivity of saline borohydrides for reduction of carboxylic esters – improved procedures for the conversion of esters to alcohols by metal borohydrides. *J. Org. Chem.,* **1982**, *47*, 4702-4708.

(5) Cainelli, G.; Galletti, P.; Giacomini, D.; Orioli, P. Solvation of the carbonyl compound as a predominant factor in the diastereofacial selectivity of nucleophilic addition. *Angew. Chem. Int. Ed.* **2000**, *39*, 523-527.

(6) Cainelli, G.; Galletti, P.; Giacomini, D. Solvent effects on stereoselectivity: more than just an environment. *Chem. Soc. Rev.* **2009**, *38*, 990-1001.

(7) Rickborn, B.; Wuesthoff, M.T. Kinetics, Stereochemistry and mechanism of sodium borohydride reduction of alkyl-substituted cyclohexanones. *J. Am. Chem. Soc.* **1970**, *92*, 6894-6904.

(8) Durand, J.; Trong Anh, N.; Huet, J. Regioselectivity in reduction by hydrides – cyclopentenone and cyclohexenone. *Tetrahedron Lett.* **1974**, *15*, 2397-2400.

(9) Pierre, J.L.; Handel, H.; Perraud, R. Fundamental role of alkaline cation in metal hydride reduction – utilization of macrocyclic coordinates .3. functional groups reduced by $LiAlH_4$. *Tetrahedron* **1975**, *31*, 2795-2798.

(10) Handel, H.; Pierre, J.L. Fundamental role of alkaline cation in metal hydride reduction – utilization of macrocyclic coordinates .4. regioselectivity and reduction of conjugated enones. *Tetrahedron*, **1975**, *31*, 2799-2802.

(11) Maruoka, K.; Itoh, T.; Sakurai, M.; Nonoshita, K.; Yamamoto, H. Amphiphilic Reactions by means of exceptionally bulky organo-aluminum reagents – rational approach for

obtaining unusual equatorial, anti-Cram and 1,4 selectivity in carbonyl alkylation. *J. Am. Chem. Soc.* **1988**, *110*, 3588-3597.

(12) *Reductions by the Alumino- and Borohydrides in Organic Synthesis;* Curran, D.P., Ed.; Wiley-VCH: New York, 1997.

(13) Lefour, J.M.; Loupy, A. Effect of cations on nucleophilic additions to carbonyl-compounds - carbonyl complexation control versus ionic association control - application to regioselectivity of addition to alpha-enones. *Tetrahedron* **1978**, *34*, 2597-2605.

(14) Loupy, A.; Seyden-Penne, J. The influence of lithium complexing agents on the regioselectivity of reductions of substituted 2-cyclohexenones by $LiAlH_4$ and $LiBH_4$. *Tetrahedron* **1980**, *36*, 1937-1942.

(15) Yadav, V.K.; Jeyaraj, D.A.; Balamurugan, R. The cation complexation model predicts the experimental pi-facial selectivity of 2-ax- and 2-eq-substituted cyclohexanones. A detailed ab initio MO investigation. *Tetrahedron* **2000**, *56*, 7581-7589.

(16) (a) Chérest, M.; Felkin, H.; Prudent, N. Torsional strain involving partial bonds. The stereochemistry of the lithium aluminium hydride reduction of some simple open-chain ketones. *Tetrahedron Lett.* **1968**, *18*, 2199-2204. (b) Chérest, M.; Felkin, H.; Prudent, N. Torsional strain involving partial bonds. The steric course of the reaction between allyl magnesium bromide and 4-t-butyl-cyclohexanone. *Tetrahedron Lett.* **1968**, *18*, 2205-2208. (c) Mengel, A.; Reiser, O. Around and beyond Cram's rule. *Chem. Rev.* **1999**, *99*, 1191-1223.

(17) (a) Wu, Y.-D.; Houk, K.N. Electronic and conformational effects on pi-facial stereoselectivity in nucleophilic additions to carbonyl-compounds. *J. Am. Chem. Soc.* **1987**, *109*, 908-910. (b) Wu, Y.-D.; Houk, K.N.; Trost, B.M. Origin of enhanced axial attack by sterically undemanding nucleophiles on cyclohexenones. *J. Am. Chem. Soc.* **1987**, *109*, 5560-5561. (c) Mukherjee, D.; Wu, Y.-D.; Fronczek, F.R.; Houk, K.N. Experimental tests of models to predict nucleophilic-addition stereochemistries. *J. Am. Chem. Soc.* **1988**, 110, 3328-3330. (d) Wu, Y.-D.; Tucker, J.A.; Houk, K.N. Stereoselectivities of nucleophilic additions to cyclohexanones substituted by polar groups – experimental investigation of reductions of trans-decalones and theoretical-studies of cyclohexanone reductions – the influence of remote electrostatic effects. *J. Am. Chem. Soc.* **1991**, *113*, 5018-5027. (e) Wu, Y.-D.; Houk, K.N.; Paddon-Row, M.N. Effect of torsional strain and electrostatic interactions on the stereochemistry of nucleophilic additions to cyclohexanone and related systems. *Angew. Chem. Int. Ed.* **1992**, *31*, 1019- 1021. (f) Paddon-Row, M.N.; Wu, Y.-D.; Houk, K.N. Electrostatic control of the stereochemistry of nucleophilic additions to substituted 7-norbornanones. *J. Am. Chem. Soc.* **1992**, *114*, 10638-10639. (g) Ando, K.; Houk, K.N.; Busch, J.; Menassé, A.; Séquin, U. Experimental and computational studies of nucleophilic additions of metal hydrides and organometallics to hindered cyclohexanones. *J. Org. Chem.* **1998**, *63*, 1761-1766.

(18) Klein, J. Electronic interpretation of stereochemistry of reduction of cyclohexanones. *Tetrahedron Lett.* **1973**, *44*, 4307-4310.

(19) Cieplak, A.S. Stereochemistry of nucleophilic-addition to cyclohexanone – the importance of 2-electron stabilizing interactions. *J. Am. Chem. Soc.* **1981**, *103*, 4540-4552.

(20) (a) Fan, Y.Y.; Gao, X.H.; Yue, J.M. Attractive natural products with strained cyclopropane and/or cyclobutene ring systems. *Sci. China Chem.* **2016**, *59*, 1126-1141. (b) Sergeiko, A.; Poroikov, V.V.; Hanus, L.O.; Dembitsky, V.M. Cyclobutane-containing alkaloids: origin, synthesis and biological activities. *Open. Med. Chem. J*. **2008**, *2*, 26-37. (c) Li, J.; Gao, K.; Bian, M.; Ding, H. Recent advances in the total synthesis of cyclobutane-containing natural products. *Org. Chem. Front.* **2020**, *7*, 136-154. (d) Li,

H.-J.; Amagata, T.; Tenney, K.; Crews, P., Additional scalarane sesterterpenes from the sponge Phyllospongia papyracea. *J. Nat. Prod*. **2007**, *70*, 802-807.

(21) (a) Manatt, S.L.; Vogel, M.; Knutson, D.; Roberts, J.D. Small-ring compounds .42. Synthesis + reactions of 3-phenyl-2-cyclobutene + some related compounds. *J. Am. Chem. Soc.* **1964**, *86*, 2645-2653. (b) Elgomati, T.; Gasteiger, J.; Lenoir, D.; Ugi, I. Stereochemical course of S_N2 reactions in cis-3-ethoxycyclobutyl and trans-3-ethoxycyclobutyl compounds. *Chem. Ber.* **1976**, *109*, 826-832. c) Dehmlow, E.V.; Büker, S. Stereoselective synthesis of 3-substituted cyclobutanols and products derived therefrom. *Chem. Ber.* **1993**, *126*, 2759-2763. (d) Nemoto, H.; Miyata, J.; Hakamata, H.; Nagamochi, M.; Fukumoto, K. A novel and efficient route to chiral A-ring aromatic trichothecanes – the first enantiocontrolled total synthesis of (-)-debromofiliformin and (-)-filiformin. *Tetrahedron* **1995**, *51*, 5511-5522. (e) Creary, X.; Kochly, E.D. gamma-Silyl cyclobutyl carbocations. *J. Org. Chem.* **2009**, *74*, 9044-9053. (f) Radchenko, D.S.; Pavlenko, S.O.; Grygorenko, O.O.; Volochnyuk, D.M.; Shishkina, S.V.; Shishkin, O.V.; Komarov, I.V. Cyclobutane-derived diamines: synthesis and molecular structure. *J. Org. Chem.* **2010**, *75*, 5941-5952. (g) Kelly, C.B.; Colthart, A.M.; Constant, B.D.; Corning, S.R.; Dubois, L.E.; Genovese, J.T.; Radziewicz, J.L.; Sletten, E.M.; Whitaker, K.R.; Tilley, L.J. Enabling the synthesis of perfluoroalkyl bicyclobutanes via 1,3 gamma-silyl elimination. *Org. Lett.* **2011**, *13*, 1646-1649. (h) Kim, J.; Wang, L.; Li, Y.; Becnel, K.D.; Frey, K.M.; Garforth, S.J.; Prasad, V.R.; Schinzai, R.F.; Liotta, D.C.; Anderson, K.S. Pre-steady state kinetic analysis of cyclobutyl derivatives of 2'-deoxyadenosine 5'-triphosphate as inhibitors of HIV-1 reverse transcriptase. *Bioorg. Med. Chem. Lett.* **2012**, *22*, 4064-4067. (i) Mitchell, L.H.; Drew, A.E.; Ribich, S.A.; Rioux, N.; Swinger, K.K.; Jacques, S.L.; Lingaraj, T.; Boriack-Sjodin, P.A.; Waters, N.J.; Wigle, T.J.; Moradei, O.; Jin, L.; Riera, T.; Porter-Scott, M.; Moyer, M.P.; Smith, J.J.; Chesworth, R.; Copeland, R.A. Aryl pyrazoles as potent inhibitors of arginine methyltransferases: identification of the first PRMT6 tool compound. *ACS Med. Chem. Lett.* **2015**, *6*, 655-659.

(22) Deraet, X.; Woller, T.; Van Lommel, R.; De Proft, F.; Verniest, G.; Alonso, M. A benchmark of density functional approximations for thermochemistry and kinetics of hydride reductions of cyclohexanones. *ChemistryOpen* **2019**, *8*, 788-806.

(23) Gaussian Revision **D01**, Frisch, M.J., Trucks, G.W., Schlegel, H.B., Scuseria, G.E., Robb, M.A., Cheeseman, J.R., Scalmani, G.,Barone, V., Petersson, G. A., Nakatsuji, H., Li, X., Caricato, M., Marenich, A., Bloino, J., Janesko, B. G., Gomperts, R., Mennucci, B., Hratchian, H. P., Ortiz, J. V., Izmaylov, A. F., Sonnenberg, J. L., Williams-Young, D., Ding, F., Lipparini, F., Egidi, F., Goings, J., Peng, B., Petrone, A., Henderson, T., Ranasinghe, D., Zakrzewski, V. G., Gao, J., Rega, N., Zheng, G., Liang, W., Hada, M., Ehara, M., Toyota, K., Fukuda, R., Hasegawa, J., Ishida, M., Nakajima, T., Honda, Y., Kitao, O., Nakai, H., Vreven, T., Throssell, K., Montgomery Jr., J. A., Peralta, J. E., Ogliaro, F., Bearpark, M., Heyd, J. J., Brothers, E., Kudin, K. N., Staroverov, V. N., Keith, T., Kobayashi, R., Normand, J., Raghavachari, K., Rendell, A., Burant, J. C., Iyengar, S. S., Tomasi, J., Cossi, M., Millam, J. M., Klene, M., Adamo, C., Cammi, R., Ochterski, J. W., Martin, R. L., Morokuma, K., Farkas, O., Foresman, J. B., and Fox, D. J., Gaussian, Inc., Wallingford CT, 2016.

(24) Grimme, S. Semiempirical hybrid density functional with perturbative second-order correlation. *J. Chem. Phys.* **2006**, *124*, 034108.

(25) Chai, J.D.; Head-Gordon, M. Long-range corrected hybrid density functionals with damped atom-atom dispersion corrections. *Phys. Chem. Chem. Phys.* **2008**, *10*, 6615-6620.

(26) Dunning, T.H. Gaussian-basis sets for use in correlated molecular calculations .1. the atoms boron through neon and hydrogen. *J. Chem. Phys.* **1989**, *90*, 1007-1023.

(27) Wheeler, S.E.; Houk, K.N. Integration Grid Errors for Meta-GGA-predicted reaction energies: origin of grid errors for the M06 suite of functionals. *J. Chem. Theory Comput.* **2010**, *6*, 395-404.

(28) Kendall, R.A.; Dunning, T.H.; Harrison, R.J. Electron-affinities of the 1st-row atoms revisited-systematic basis-sets and wave-functions. *J. Chem. Phys.* **1992**, *96*, 6796-6806.

(29) (a) Grimme, S.; Antony, J.; Ehrlich, S.; Krieg, H. A consistent and accurate ab initio parametrization of density functional dispersion correction (DFT-D) for the 94 elements H-Pu. *J. Chem. Phys.* **2010**, *132*, 154104. (b) Grimme, S.; Ehrlich, S.; Goerigk, L. Effect of the damping function in dispersion corrected density functional theory. *J. Comput. Chem.* **2011**, *32*, 1456-1465.

(30) Rassolov, V.A.; Ratner, M.A.; Pople, J.A.; Redfern, P.C.; Curtiss, L.A. 6-31G* basis set for third-row atoms. *J. Comp. Chem.* **2001**, *22*, 976-984.

(31) Blaudeau, J.; McGrath, M.P.; Curtiss, L.A.; Radom, L. Extension of Gaussian-2 (G2) theory to molecules containing third-row atoms K and Ca. *J. Chem. Phys.* **1997**, *107*, 5016-5021.

(32) Marenich, A.V.; Cramer, C.J.; Truhlar, D.G. Universal solvation model based on solute electron density and on a continuum model of the solvent defined by the bulk dielectric constant and atomic surface tensions. *J. Phys. Chem. B* **2009**, *113*, 6378-6396.

(33) (a) Lee, C.; Yang, W.; Parr, R.G. Development of the Colle-Salvetti correlation-energy formula into a functional of the electron-density. *Phys. Rev. B* **1988**, *37*, 785. (b) Becke, A.D. A new mixing of Hartree-Fock and local density-functional theories. *J. Chem. Phys.* **1993**, *98*, 1372.

(34) Zhao, Y.; Truhlar, D.G. The M06 suite of density functionals for main group thermochemistry, thermochemical kinetics, noncovalent interactions, excited states, and transition elements: two new functionals and systematic testing of four M06-class functionals and 12 other functionals. *Theor. Chem. Acc.* **2008**, *120*, 215.

(35) Johnson, E.R.; Keinan, S.; Mori-Sanchez, P.; Contreras-Garcia, J.; Cohen, A.J.; Yang, W. Revealing noncovalent interactions. *J. Am. Chem. Soc.* **2010**, *132*, 6498-6506.

(36) Contreras-Garcia, J.; Johnson, E.R.; Keinan, S.; Chaudret, R.; Piquemal, J.-P.; Beratan, D.N.; Yang, W. NCIPLOT: A program for plotting noncovalent interaction regions. *J. Chem. Theory Comput.* **2011**, *7*, 625-632.

(37) Humphrey, W.; Dalke, A.; Schulten, K. VMD: Visual molecular dynamics. *J. Mol. Graph.* **1996**, *14*, 33-38.

(38) Contreras-Garcia, J.; Boto, R.A.; Izquierdo-Ruiz, F.; Reva, I.; Woller, T.; Alonso, M. A benchmark for the non-covalent interaction (NCI) index or … is it really all in the geometry?. *Theor. Chem. Acc.* **2016**, *135*, 242.

(39) ^{1}H-NMR spectra available on https://www.pharmablock.com/ (accessed Nov 15, 2019).

(40) (a) Dauben, W.G.; Fonken, G.J.; Noyce, D.S. The stereochemistry of hydride reductions. *J. Am. Chem. Soc.* **1956**, *78*, 2579-2582. (b) Neufeldt, S.R.; Jiménez-Osés, G.; Comins, D.L.; Houk, K.N. A twist on facial selectivity of hydride reductions of cyclic ketones: twist-boat conformers in cyclohexanone, piperidone and tropinone reactions. *J. Org. Chem.* **2014**, *79*, 11609-11618.

(41) (a) Luibrand, R.T.; Taigounov, I.R.; Taigounov, A.A. A theoretical study of the reaction of lithium aluminium hydride with formaldehyde and cyclohexanone. *J. Org. Chem.* **2001**, *66*, 7254-7262. (b) Bocca, C.C.; Basso, E.A.; Gauze, G.F. Substituent effects on the reduction of 2-OMe, 2-SMe and 2-SeMe cyclohexanones by $LiAlH_4$: an investigation of conformational equilibrium and transition states. *Chem. Phys. Lett.* **2005**, *413*, 434-439. (c) Bocca, C.C.; Rittner, R.; da Silva, A.P.; Basso, E.A. Substituent

effects on the reduction of 2-alkylcyclohexanones by LiAlH4: an investigation of conformational equilibria and transition states. *J. Phys. Org. Chem.* **2011**, *24*, 241-248.

(42) Bürgi, H.B.; Dunitz, J.D.; Lehn, J.M.; Wipff, G. Stereochemistry of reaction paths at carbonyl centers. *Tetrahedron* **1974**, *30*, 1563-1572.

(43) (a) Vansteenkiste, P.; Van Speybroeck, V.; Verniest, G.; De Kimpe, N.; Waroquier, M. Applicability of the hindered rotor scheme to the puckering mode in four-membered rings. *J. Phys. Chem. A* **2006**, *110*, 3838-3844. (b) Vansteenkiste, P.; Van Speybroeck, V.; Verniest, G.; De Kimpe, N.; Waroquier, M. Four-membered heterocycles with a carbon-heteroatom exocyclic double bond at the 3-position: puckering potential and thermodynamic properties. *J. Phys. Chem. A* **2007**, *111*, 2797-2803.

(44) (a) Ashby, E.C.; Boone, J.R. Stereochemistry of reductions of ketones by simple and complex metal hydrides of the main group elements. *J. Org. Chem.* **1976**, *41*, 2890-2902. (b) Nakata, T.; Tani Y.; Hatozaki, M.; Oishi, T. Stereoselective reduction of α-methyl-β-hydroxy ketones with zinc borohydride. *Chem. Pharm. Bull.* **1983**, *32*, 1411-1415. (c) Cabral, S.; Hulin, B.; Kawai, M. Lithium borohydride: a reagent of choice for the selective reductive amination of cyclohexanones. *Tetrahedron Lett.* **2007**, *48*, 7134-7136. (d) Esteve, J.; Matas, S.; Pellicena, M.; Velasco, J.; Romea, P.; Urpi, F.; Font-Bardia, M. Highly stereoselective synthesis of syn-1,3-diols through a sequential titanium-mediated aldol reaction and $LiBH_4$ reduction. *Eur. J. Org. Chem.* **2010**, 3146-3151.

(45) Skyner, R.E.; McDonagh, J.L.; Groom, C.R.; van Mourik, T.; Mitchell, J.B.O. A review of methods for the calculation of solution free energies and the modelling of systems in solution. *Phys. Chem. Chem. Phys.* **2015**, *17*, 6174-6191.

(46) CYLview, 1.0b, C.Y. Legault, Université de Sherbrooke, **2009**.

Table of Contents (TOC)